Growth of spatial correlations in the aging of a simple structural glass

Azita Parsaeian and Horacio E. Castillo

Department of Physics and Astronomy, Ohio University, Athens, Ohio 45701, USA

We present a detailed numerical study of dynamical heterogeneities in the aging regime of a simple binary Lennard-Jones glass former. For most waiting times t_w and final times t, both the dynamical susceptibility $\chi_4(t,t_w)$ and the dynamical correlation length $\xi_4(t,t_w)$ can be approximated as products of two factors: (i) a waiting-time-dependent scale that grows as a power of t_w, and (ii) a scaling function dependent on t,t_w only through the value of the intermediate scattering function $C(t,t_w)$. We find that $\chi_4(t,t_w)$ is determined only in part by the correlation volume.

When a liquid's temperature is rapidly reduced, it can become supercooled and eventually undergo a transition into a glass state. As the transition is approached, the relaxation time and the viscosity grow by several orders of magnitude. The glass transition is the point at which the relaxation time of the liquid becomes longer than a fixed laboratory time scale [1]. Consequently, a system in the glass state is out of thermodynamic equilibrium. In particular, *physical aging* is observed: *time translation invariance (TTI)* is broken, i.e., correlations between observables at times t_w (the *waiting time*) and t (the *final time*) depend nontrivially on both times, and not just on their difference $t-t_w$ [2].

Several observations about the glass transition, including the rapidly increasing relaxation time scales, the presence of nonexponential relaxation, and the violation of Stokes-Einstein relations between viscosity and diffusivity, have motivated the assumption that *dynamical heterogeneities* are present in the supercooled liquid [1,3,4]. Dynamical heterogeneities are nanometer-scale regions containing molecules that rearrange cooperatively at very different rates compared to the bulk [3,4]. More recently, dynamical heterogeneities have been directly observed in local probe experiments in supercooled liquids [5,6], glasses [7–9], and granular systems near the jamming transition [10]. However, except for the pioneering work by Parisi [11], most simulations studying dynamical heterogeneities in off-lattice models of structural glasses have focused on the supercooled regime [12–19].

In this Rapid Communication we present a simulation study of dynamic spatial correlations of a continuous-space, quasirealistic glass model in the aging regime, with the goal of characterizing their extent, space dependence, and time dependence. We discuss the spatial correlations of density fluctuations, which have been used before to characterize dynamical heterogeneities in the supercooled regime [13,15]. We first present detailed results from an isotropic probe, which allows us to focus on the strength and spatial extent of the correlations, and later on briefly discuss the case of an anisotropic probe, which permits studying the geometry of the correlated region. A theoretical framework that postulates the presence of local fluctuations in the age of the sample [21,22] predicts that probability distributions of local fluctuations in the aging regime are approximately independent of t_w at fixed values of the two-time global correlation $C_{global}(t,t_w)$. This prediction has been confirmed in simula-

tions of both spin glasses [22] and structural glasses [23] (where C_{global} is the self-part of the intermediate scattering function). Motivated by this scaling, we examine the possible presence of scaling behavior as a function of C_{global} and t_w in the dynamic spatial correlations.

In order to probe the spatial density correlations, we use the four-point (two-time, two-position) correlation function [13]:

$$g_4(\mathbf{r},t,t_w) = \frac{1}{N\rho}\left\langle \sum_{ik} \delta[\mathbf{r}-\mathbf{r}_k(t_w)+\mathbf{r}_i(t_w)]w[|\mathbf{r}_i(t)-\mathbf{r}_i(t_w)|] \right.$$
$$\left. \times w[|\mathbf{r}_k(t)-\mathbf{r}_k(t_w)|] \right\rangle - \left\langle \frac{Q(t,t_w)}{N} \right\rangle^2; \quad (1)$$

where $Q(t,t_w) \equiv \Sigma_{i=1}^{N} w[|\mathbf{r}_i(t_w)-\mathbf{r}_i(t)|]$ and $w(|\mathbf{r}_1-\mathbf{r}_2|)$ is an overlap function which is unity for $|\mathbf{r}_1-\mathbf{r}_2| \leq a$ and zero otherwise. ($a \equiv 0.3\sigma_{AA}$ is an upper bound for the typical amplitude of the vibrational motion [13].) By integrating $g_4(\mathbf{r},t,t_w)$ over space, the generalized four-point density susceptibility $\chi_4 \equiv \int d^3\mathbf{r}\, g_4(\mathbf{r},t,t_w)$ [13] is obtained. The self-part of the intermediate scattering function $C=C_{global}(t,t_w)$ $=(1/N)\Sigma_{j=1}^{N} \exp\{i\mathbf{q}\cdot[\mathbf{r}_j(t)-\mathbf{r}_j(t_w)]\}$ can be used as a measure of the correlation between the configurations of the system at times t_w and t: it is unity when $t=t_w$ and decays to zero when $t-t_w \gg t_w$ [1,2,20].

We performed 4000 independent molecular dynamics runs for the binary Lennard-Jones (LJ) system of Ref. [20], which has a mode coupling critical temperature $T_c=0.435$. A system of 8000 particles was equilibrated at a temperature $T_0=5.0$, then instantly quenched to $T=0.4$, and then allowed to evolve at that temperature for 2.5×10^3 Lennard-Jones time units. The origin of times was taken at the instant of the quench. After the quench, data were taken at times in a geometric sequence $t_n=t_0 r^n$ (with $n=0,\ldots,61$, $t_0=10$, $r=10^{1/25} \approx 1.09$).

We first discuss the four-point density susceptibility χ_4. In the top panel of Fig. 1 we see that for fixed waiting time t_w, as the time difference $t-t_w$ increases, the spatial correlation increases until it reaches a maximum, and then decreases. The value of the correlation χ_4 at the peak and the time difference $t-t_w$ at which the peak occurs both grow as a function of t_w. Analogous behaviors are observed in numerical simulations of supercooled liquids (see, e.g., Refs.
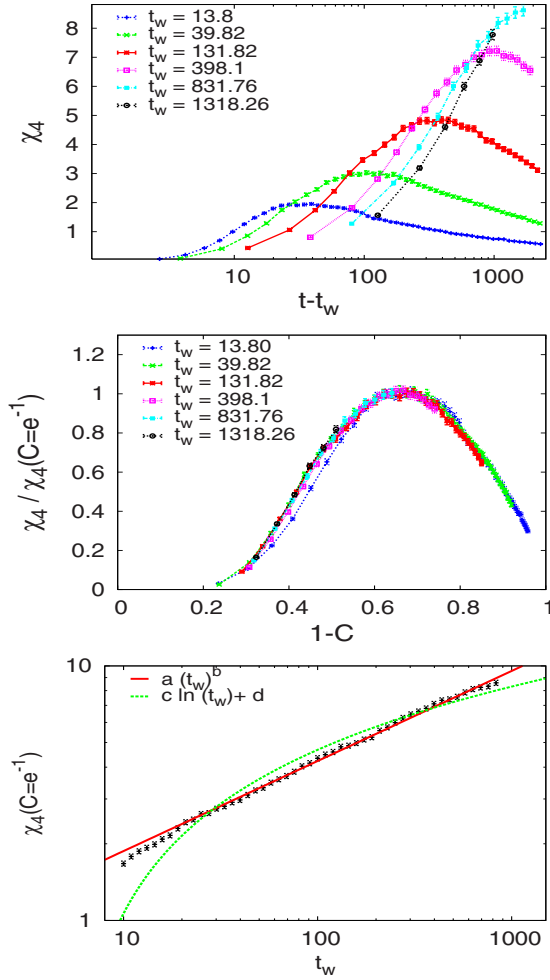
FIG. 1. (Color online) Top panel: Generalized density suscepti-bility χ_4 as a function of the time difference $t-t_w$, for waiting times $t_w = 13.8, \ldots, 1318.26$. Middle panel: Rescaled density susceptibility versus $1-C$, for the same waiting times. Bottom panel: Rescaling factor of the density susceptibility, $\chi_4(C=1/e)$, versus the waiting time. The straight line is a fit to $\chi_4(C=1/e)=at_w^b$, with fitting parameters $b=0.353\pm0.003$ and $a=0.83\pm0.02$. The curved line is a logarithmic fit $\xi_4(C=1/e)=c\ln(t_w)+d$, with parameters $c=1.57\pm0.04$ and $d=-2.6\pm0.2$. Statistical errors are shown by error bars in the data for all three panels.

[13,15]) as the temperature is decreased; and in experiments in two-dimensional granular systems [10], as the area fraction is increased. As we anticipated above, we test for a possible scaling behavior with $C=C_{\text{global}}$ by plotting, in the middle panel of Fig. 1, the rescaled quantity $\chi_4/\chi_4(C=1/e)$ as a function of $1-C$. We observe that all curves approximately collapse onto a single master curve. Thus we can say that $\chi_4(t,t_w) \approx \chi_4^0(t_w)\phi(C(t,t_w))$, where $\chi_4^0(t_w) \equiv \chi_4(t,t_w)|_{C(t,t_w)=1/e}$; a rescaling factor that depends only on t_w, and $\phi(C(t,t_w))$ is a scaling function which depends on times only through the value of the intermediate scattering function $C(t,t_w)$. As we see in the bottom panel of Fig. 1, the rescaling factor as a function of t_w can be fitted with the power law form $\chi_4^0(t_w)=at_w^b$, with the power $b=0.353\pm0.003$ [25]. As the figure shows, this fit is much better than a fit to a logarithmic form $c\ln(t_w)+d$.

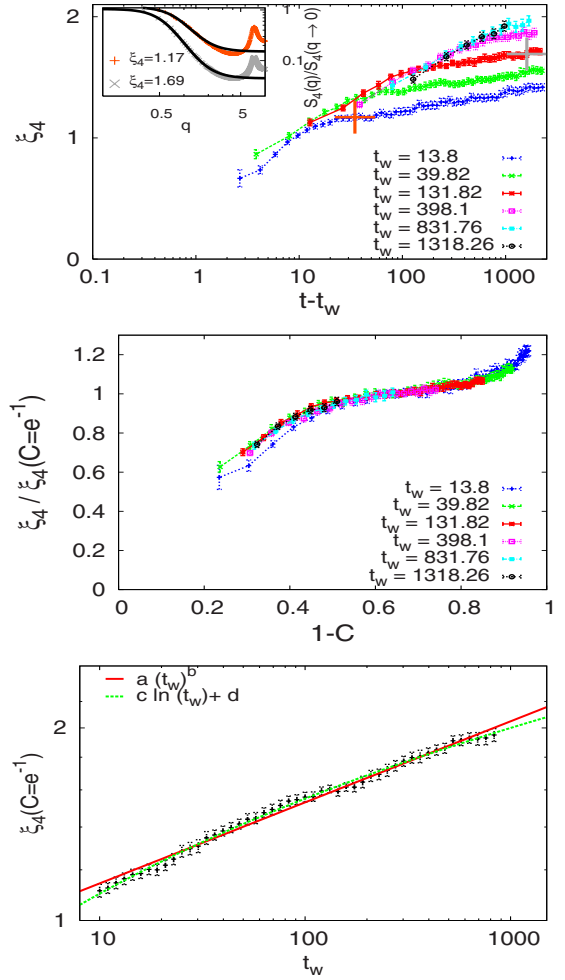FIG. 2. (Color online) Top panel inset: Rescaled $S_4(q,t,t_w)$ as a function of q for two (t_w,t) pairs, with low-q fits shown (dashed lines). The correlation lengths extracted from the fits are indicated in the key. Top panel: Correlation length as a function of $t-t_w$ for various t_w's. The $+$ represent the $(t-t_w,\xi_4)$ values for the two curves in the inset. Middle panel: Rescaled ξ_4 versus $1-C$. Bottom panel: Rescaling factor of the correlation length, $\xi_4(C=1/e)$, versus t_w. The straight line is a fit to $\xi_4(C=1/e)=a(t_w)^b$, with parameters $a=0.853\pm0.007$ and $b=0.126\pm0.001$. The other line is a logarithmic fit, $\xi_4(C=1/e)=c\ln(t_w)+d$, with parameters $c=0.195\pm0.001$ and $d=0.651\pm0.008$. Statistical errors are shown by error bars in the data for all three panels.

We now extract a dynamic correlation length $\xi_4(t,t_w)$ from our data. By Fourier transforming the correlation function $g_4(\mathbf{r},t,t_w)$ we obtain the four-point dynamic structure factor $S_4(\mathbf{q},t,t_w)$ [13,15,17]. We fit its small-q behavior with an empirical scaling form [15]: $S_4(\mathbf{q})=(S_4^0-K)f(\xi_4|\mathbf{q}|)+K$, with $f(x)\equiv1/(1+x^\gamma)$. Choosing $\gamma=2$ would give an Ornstein-Zernicke (OZ) form, but there is theoretical evidence [24] that the OZ form may not be a good description of $S_4(\mathbf{q})$, and in fact $\gamma=2.9\pm0.1$ provides substantially better fits to our data [24]. Since the $\mathbf{q}$-dependent part of $S_4(\mathbf{q})$ scales with $\xi_4|\mathbf{q}|$, and its value is reduced from its maximum at $|\mathbf{q}|=0$ to half of its maximum at $|\mathbf{q}|=1/\xi_4$, we interpret ξ_4 as a correlation length. The fits are performed in the range $0.4\leqslant q\leqslant1.9$, for 175 curves corresponding to all the time
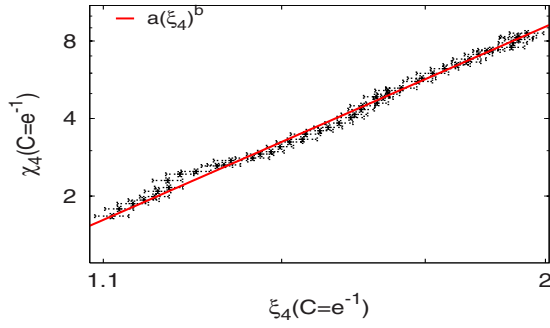
FIG. 3. (Color online) Four-point density susceptibility rescaling factor versus the dynamic correlation length rescaling factor. The straight line corresponds to $a(\xi_4)^b$, with $b=2.89\pm0.03$ and $a=1.23\pm0.02$. Statistical errors for both abscissa and ordinate are shown for all the data points.

pairs shown in Fig. 2. The fitting parameters $S_4^0(t,t_w)$, $\xi_4(t,t_w)$, and $K(t,t_w)$ are determined independently for each time pair (t,t_w). The scaling function $f(x)$ is not allowed to change with (t,t_w): the (t,t_w)-independent empirical parameter γ is determined by minimizing the average square error over the whole set of fits. The maximum difference between the data and the corresponding fits never exceeds 7.5% [26]. Two typical fits are shown in the inset of the top panel of Fig. 2.

The top panel of Fig. 2 shows the correlation length ξ_4 as a function of the time difference $t-t_w$ for $t_w = 13.8,\ldots,1318.26$. We see two regimes in this plot: (i) an early aging regime [27] ($t-t_w \lesssim t_w$), where ξ_4 is approximately time-translation invariant (i.e., it depends on $t-t_w$ but not on t_w), and (ii) a late aging regime ($t-t_w \gtrsim t_w$), where ξ_4 generally grows with increasing t_w at fixed $t-t_w$. This increase of ξ_4 with t_w is analogous to its increase in supercooled liquids as the temperature is lowered [13,28].

We find that ξ_4 always grows as a function of $t-t_w$, at fixed waiting time t_w. Simulations in the supercooled regime show divergent results on this issue: in Ref. [13] the correlation length increases initially, reaches a maximum, and goes to zero for long time differences, while in Refs. [15,18] the correlation length always grows with time difference. Similar to χ_4, the correlation length ξ_4 also displays an ap-

proximate scaling behavior with C_{global}: in the middle panel of Fig. 2, we plot $\xi_4/\xi_4(C=1/e)$ as a function of $1-C$. The curves collapse onto a single master curve and we can conclude that $\xi_4(t,t_w) \approx \xi_4^0(t_w)\varphi(C(t,t_w))$, where $\xi_4^0(t_w) \equiv \xi_4(t,t_w)|_{C(t,t_w)=1/e}$. In the bottom panel of Fig. 2, we observe that the dependence of the scaling factor $\xi_4^0(t_w)$ on t_w can be fitted roughly equally well by a power law form $\xi_4^0(t_w)=a(t_w)^b$ where $b=0.126\pm0.001$ [11]; or by a logarithmic form $\xi_4^0(t_w)=c\ln(t_w)+d$. However, the power law form seems preferable because it is consistent with the physically motivated scaling $\chi_4^0 \sim (\xi_4^0)^b$ found below.

To test whether the value of $\chi_4(t,t_w)$ is controlled by the correlation volume $[\xi_4(t,t_w)]^3$, in Fig. 3 we plot the susceptibility scaling factor $\chi_4^0(t_w)$ as a function of the correlation length scaling factor $\xi_4^0(t_w)$, and find that the data are indeed well represented by a power law form with a power close to 3: $\chi_4^0 \propto (\xi_4^0)^b$ with $b=2.89\pm0.03$ (see also Ref. [11]). However, looking at the data in more detail reveals an additional variation of $\chi_4(t,t_w)$ that cannot be due to the correlation volume: if we compare the two plots of $\chi_4(t,t_w)$ and $\xi_4(t,t_w)$ versus the global correlation $C(t,t_w)$ at constant t_w (the middle panels of Figs. 1 and 2), we find that, as $C(t,t_w) \to 0$, $\chi_4(t,t_w)$ almost reaches zero, but $\xi_4(t,t_w)$ increases. Clearly, the evolution of χ_4 at constant t_w is controlled not only by the correlation length but also by the amplitude of the correlations.

We now briefly turn our attention to the anisotropic spatial structure of the correlations [17–19]. We define a spatial correlator $\mathcal{G}_4(\mathbf{r},\mathbf{k},t,t_w)$ by replacing, in the definition of $g_4(\mathbf{r},t,t_w)$, all occurrences of $w[|\mathbf{r}(t)-\mathbf{r}(t_w)|]$ with the anisotropic function $\cos\{\mathbf{k}\cdot[\mathbf{r}(t)-\mathbf{r}(t_w)]\}$ [23]. We choose $\mathbf{k}=(6.68,0.00,2.67)$, with $|\mathbf{k}|=7.2$, i.e., at the peak of the static structure function $S(k)$. The Fourier transform of $\mathcal{G}_4(\mathbf{r},\mathbf{k},t,t_w)$ with respect to $\mathbf{r}$ is the four-point anisotropic dynamic structure factor $\mathcal{S}_4(\mathbf{q},\mathbf{k},t,t_w)$ [19]. As we see in the left panel of Fig. 4, this four-point function is indeed anisotropic: the contours of constant $\mathcal{S}_4$ extend further in the q_y direction than in the q_x direction. We fitted $\mathcal{S}_4$ with an empirical form which generalizes the isotropic one: $\mathcal{S}_4=(\mathcal{S}_4^0-K)f([(q_x\xi_{4,x})^2+(q_y\xi_{4,y})^2]^{1/2})+K$, with $f(x)=1/(1+x^\gamma)$. Here $\mathcal{S}_4^0, K, \xi_{4,x}$, and $\xi_{4,y}$ are (t,t_w)-dependent fitting parameters, and $\gamma=3.4\pm0.1$ [independent of (t,t_w)] is determined by a
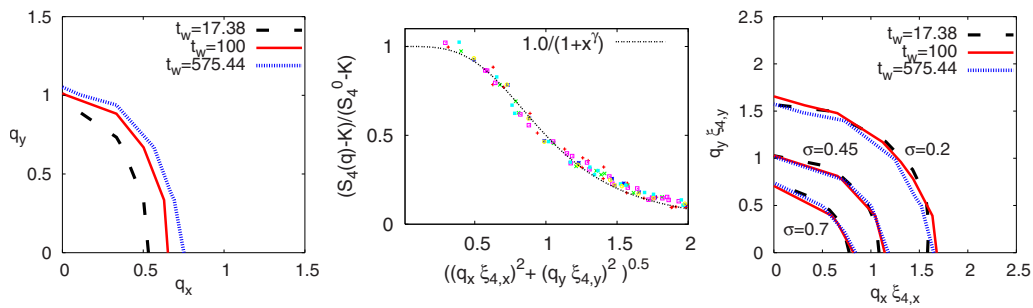

FIG. 4. (Color online) Left panel: Contours for constant $\mathcal{S}_4(\mathbf{q},\mathbf{k},t,t_w)$, plotted as a function of the q_x and q_y coordinates, for $q_z=0$, waiting times $t_w=17.38,100,575.44$, and constant $C_{\text{global}}=0.3$. The correlations extend more in the q_y direction than in the q_x direction. Middle panel: Rescaled four-point function $\sigma(\mathbf{q},\mathbf{k},t,t_w)$ for six time pairs, for $t_w=17.38,100,575.44$, and $C_{\text{global}}=0.3,0.5$. All of the rescaled data approximately collapse onto one curve which is fairly well fitted by the scaling form $1/(1+x^\gamma)$. Right panel: Contours of constant $\sigma(\mathbf{q},\mathbf{k},t,t_w)=0.2,0.45,0.7$, plotted as a function of the rescaled wave vector $(\xi_{4,x}q_x,\xi_{4,y}q_y)$, for three time pairs $t_w=17.38,100,575.44$ with $C_{\text{global}}=0.3$.

global fit to all the data shown in Fig. 4. The middle panel of Fig. 4 shows that the rescaled quantity $\sigma(\mathbf{q}, \mathbf{k}, t, t_w)$ $\equiv [\mathcal{S}_4(\mathbf{q}, \mathbf{k}, t, t_w) - K(t, t_w)]/[\mathcal{S}_4^0(t, t_w) - K(t, t_w)]$, computed for six time pairs, collapses onto one curve that agrees well with $f(x)$. The right panel of Fig. 4 shows a contour plot of $\sigma(\mathbf{q}, \mathbf{k}, t, t_w)$. Here the contours for various time pairs collapse, as long as σ is kept constant and rescaled wave vector components $\xi_{4,x} q_x$ and $\xi_{4,y} q_y$ are used on the axes. Since $k_y = 0$, and $q_z = 0$, $\mathcal{S}_4(\mathbf{q}, \mathbf{k}, t, t_w)$ is probing correlations between displacements in the x direction. We find that $\xi_{4,x}(t, t_w) > \xi_{4,y}(t, t_w)$, i.e., the correlation extends further along the direction of the probed displacements than along the perpendicular direction, and we interpret this as a manifestation of cooperative "stringlike" motion, as in the supercooled regime [17–19].

In summary, we have studied the aging regime of a simple glass-forming model and found evidence of scaling for the dynamical susceptibility $\chi_4(t, t_w)$ and the dynamical correlation length $\xi_4(t, t_w)$ as products of a power of t_w times a scaling function that depends on times only through $C_{\text{global}}(t, t_w)$. Additionally, we have found evidence of time-independent scaling functions that describe the $\mathbf{q}$ dependence of both the isotropic and the anisotropic dynamic structure factors. In the anisotropic case, we have found evidence for stringlike motion, similar to the one observed in supercooled liquids.

[1] P. Debenedetti and F. Stillinger, Nature (London) **410**, 259 (2001).

[2] J.-P. Bouchaud, L. F. Cugliandolo, J. Kurchan, and M. Mézard, in *Spin Glasses and Random Fields*, edited by A. P. Young (World Scientific, Singapore, 1998).

[3] M. D. Ediger, Annu. Rev. Phys. Chem. **51**, 99 (2000).

[4] H. Sillescu, J. Non-Cryst. Solids **243**, 81 (1999).

[5] W. K. Kegel and A. V. Blaaderen, Science **287**, 290 (2000).

[6] E. R. Weeks *et al.*, Science **287**, 627 (2000).

[7] R. Courtland and E. Weeks, J. Phys.: Condens. Matter **15**, S359 (2003).

[8] E. Vidal-Russell and N. E. Israeloff, Nature (London) **408**, 695 (2000); K. S. Sinnathamby, H. Oukris, and N. E. Israeloff, Phys. Rev. Lett. **95**, 067205 (2005).

[9] P. Wang, C. Song, and H. A. Makse, Nat. Phys. **2**, 526 (2006).

[10] O. Dauchot, G. Marty, and G. Biroli, Phys. Rev. Lett. **95**, 265701 (2005); A. R. Abate and D. J. Durian, Phys. Rev. E **76**, 021306 (2007).

[11] G. Parisi, J. Phys. Chem. B **103**, 4128 (1999).

[12] W. Kob, C. Donati, S. J. Plimpton, P. H. Poole, and S. C. Glotzer, Phys. Rev. Lett. **79**, 2827 (1997).

[13] N. Lacevic, F. W. Starr, T. B. Schroder, and S. C. Glotzer, J. Chem. Phys. **119**, 7372 (2003).

[14] R. Yamamoto and A. Onuki, Phys. Rev. E **58**, 3515 (1998).

[15] C. Toninelli, M. Wyart, L. Berthier, G. Biroli, and J. P. Bouchaud, Phys. Rev. E **71**, 041505 (2005).

[16] S. Whitelam, L. Berthier, and J. P. Garrahan, Phys. Rev. Lett. **92**, 185705 (2004).

[17] C. Donati *et al.*, Phys. Rev. Lett. **80**, 2338 (1998).

[18] B. Doliwa and A. Heuer, Phys. Rev. E **61**, 6898 (2000).

[19] E. Flenner and G. Szamel, J. Phys.: Condens. Matter **19**, 205125 (2007).

[20] W. Kob and J. L. Barrat, Phys. Rev. Lett. **78**, 4581 (1997).

[21] C. Chamon, M. P. Kennett, H. E. Castillo, and L. F. Cugliandolo, Phys. Rev. Lett. **89**, 217201 (2002).

[22] H. E. Castillo, C. Chamon, L. F. Cugliandolo, and M. P. Kennett, Phys. Rev. Lett. **88**, 237201 (2002); H. E. Castillo, C. Chamon, L. F. Cugliandolo, J. L. Iguain, and M. P. Kennett, Phys. Rev. B **68**, 134442 (2003); C. Chamon, P. Charbonneau, L. F. Cugliandolo, D. R. Reichman, and M. Sellitto, J. Chem. Phys. **121**, 10120 (2004).

[23] H. E. Castillo and A. Parsaeian, Nat. Phys. **3**, 26 (2007).

[24] G. Biroli, J. P. Bouchaud, K. Miyazaki, and D. R. Reichman, Phys. Rev. Lett. **97**, 195701 (2006).

[25] In our data [26] $\tau_\alpha(t_w) \sim t_w^{0.9}$, which leads to $\chi_4 \sim [\tau(t_w)]^{0.4}$. For a supercooled LJ system $\chi_4 \sim [\tau(T)]^{0.4}$ was found [16].

[26] A. Parsaeian and H. E. Castillo (unpublished).

[27] For small enough $t - t_w$, $C_{\text{global}}(t, t_w)$ should be TTI (i.e., no aging), but in our data time separations are too large to observe this regime.

[28] L. Berthier *et al.*, Science **310**, 1797 (2005).